ACS OMEGA

Open Access
This article is licensed under CC-BY-NC-ND 4.0

http://pubs.acs.org/journal/acsodf
Article

Flexible Monolithic Bifunctional Device Based on a Lift-off (In,Ga)N Film for Both Lighting and Self-Driven Detection

Binbin Hou, Qianyi Zhang, Jianya Zhang, Renjun Pei,* and Yukun Zhao*

Cite This: *ACS Omega* 2024, 9, 8117−8122

Read Online

ACCESS | Metrics & More | Article Recommendations | Supporting Information

ABSTRACT: Although flexible monolithic bifunctional devices are significant for next-generation optoelectronic devices, it is quite challenging to realize them. In this work, a flexible monolithic device with both functions of emission and self-driven detection has been proposed and demonstrated successfully. By a quick electrochemical etching method, the device is created using a lift-off (In,Ga)N film detaching from the epitaxial silicon substrate. The Si removal is beneficial for releasing stress and reducing the internal polarization effects under bending conditions, keeping the electroluminescence peak wavelength quite stable. With good flexibility, the monolithic bifunctional device can maintain both stable detection and emission performance under bending conditions. Furthermore, two functions of detection and lighting of the flexible monolithic device can not only be realized separately but also simultaneously. This means that the flexible monolithic device can detect and emit light at the same time. With the advantages of miniaturization and multifunctionality, this work paves an effective way to develop new monolithic multifunctional devices for both self-driven detection and wearable intelligent display.

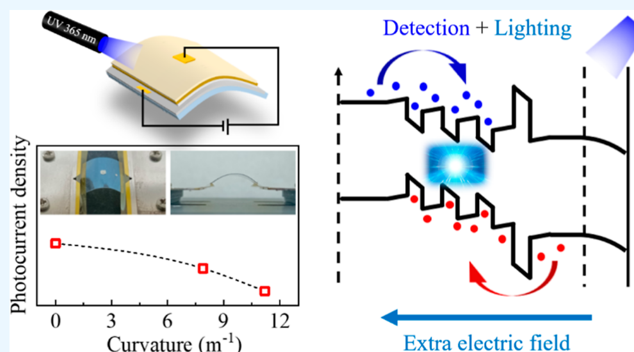

1. INTRODUCTION

Light-emitting diodes (LEDs) are highly energy-efficient and long-lasting, making them ideal for various applications such as indoor and outdoor lighting.[1−3] With the advantage of ultralow energy consumption, self-driven photodetectors (PDs) are the indispensable devices in various applications, such as optical communications, remote sensing, industrial automation, and environmental monitoring.[4] Self-driven nanotechnology aims at building a self-driven system that operates independently, sustainably and wirelessly.[5] In general, the dual functions of photoemission and detection are operated by two separate devices of LED and PD rather than a single monolithic device, which requires additional power supply equipment, making the system more cumbersome and expensive.[6−8] Furthermore, the monolithic device can greatly enhance the adaptability and largely reduce the volume and weight of the system.[9] Hence, due to the increasing demand for multifunctionality, portability, and miniaturization, the ability of integrating the PD and LED into a single monolithic device is essential for the next-generation optoelectronic devices.[9,10]

In addition, the (In,Ga)N materials have the advantages of long lifetime and small size,[1−3] as well as the direct and tunable band gap.[11] However, the general epitaxial substrates for growing (In,Ga)N materials are rigid, which means that they are quite difficult to be used for preparing flexible devices.[12,13] Furthermore, because of withstanding large mechanical deformation under bending conditions,[14] the preparation processes for the flexible monolithic bifunctional device are easily damaged. In general, some conventional integrated devices are often realized by transceiver separation chips, which have some problems such as low efficiency, weak compactness and poor robustness.[15] Therefore, it is still very attractive but extremely challenging to realize a single-piece flexible device with both functions of emission and self-driven detection.[16]

In our previous works, we proposed an electrochemical (EC) etching method to detach GaN-based materials.[17,18] In this work, we detach the (In,Ga)N film from the original Si substrate by the EC method and transfer it to a flexible, conductive substrate. The flexible conductive substrate was obtained by sputtering indium−tin oxide (ITO) on a polyethylene terephthalate (PET) substrate. Then a flexible monolithic bifunctional device is fabricated successfully based on the lift-off (In,Ga)N film. The light response performance under different incident light powers and the influence of the flexible substrate on the detection and emission performance of the device are investigated. Importantly, the two functions of detection and lighting are realized simultaneously for the

Received: October 27, 2023
Revised: January 15, 2024
Accepted: January 24, 2024
Published: February 3, 2024

© 2024 The Authors. Published by American Chemical Society

https://doi.org/10.1021/acsomega.3c08503
ACS Omega 2024, 9, 8117−8122

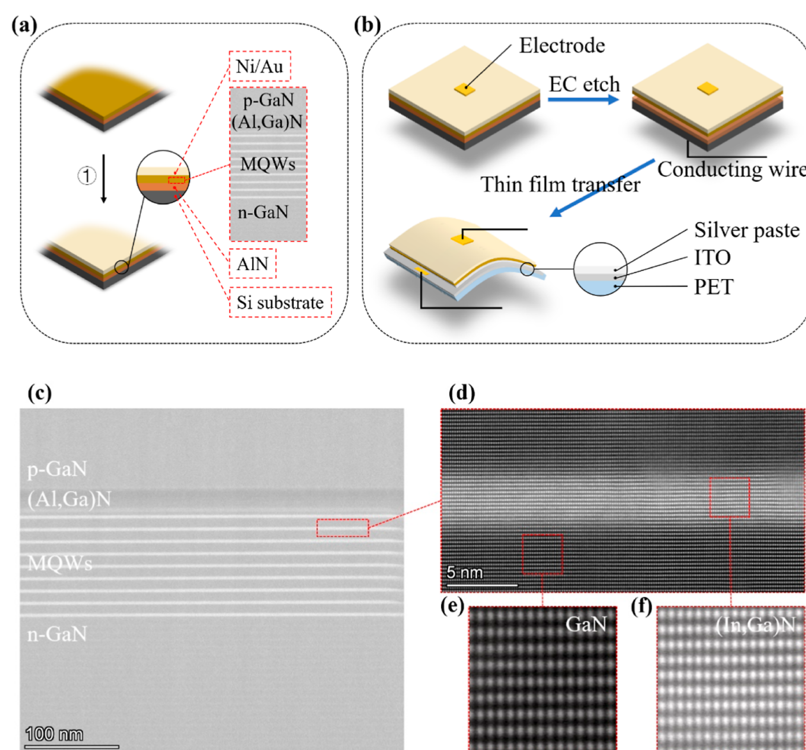

Figure 1. (a) Epitaxial structure of (In,Ga)N thin films. (b) Flowchart of preparing the flexible device. (c) Side view STEM image of the GaN-based film after EC etching. (d) Enlarged STEM image of the (In,Ga)N/GaN MQWs. AC-STEM images of the (e) GaN and (f) (In,Ga)N crystals.

flexible monolithic device. This work provides a valuable approach to develop flexible detection and emission monolithic devices.

2. EXPERIMENTAL PROCEDURE

2.1. Preparation of the (In,Ga)N Film. In Figure 1a, we grew the GaN-based epitaxial structure on Si (111) using metal organic chemical vapor deposition (MOCVD). Following the growth direction, the epitaxial structure includes an AlN nucleation layer [~330 nm, T_G (growth temperature) ≈ 1080 °C], a (Al,Ga)N multilayer buffer (~600 nm, T_G ≈ 1050 °C), an unintentionally doped GaN layer (~800 nm, T_G = 1020 °C), and a Si-doped n-GaN layer (~2800 nm, [Si] ≈ 8 × 10^{18} cm^{-3}; T_G ≈ 1020 °C). It is followed by 9-period (In,Ga)N/GaN multiple quantum wells (MQWs) of approximately 3/9 nm (T_G ≈ 750 °C), a Mg-doped p-(Al,Ga)N electron-blocking layer (EBL) of ~30 nm ([Mg] ≈ 1 × 10^{20} cm^{-3}; T_G ≈ 940 °C), a Mg-doped p-GaN layer (~60 nm, [Mg] ≈ 3 × 10^{19} cm^{-3}; T_G ≈ 940 °C), and a heavily Mg-doped p-GaN contact layer (~20 nm, [Mg] ≈ 2 × 10^{20} cm^{-3}; T_G ≈ 940 °C).

After MOCVD growth, 5 nm/5 nm Ni/Au metal was deposited on the surface of the 2 in. sample to prepare the current spreading layer (① in Figure 1a). The sample was divided into 15 × 15 mm sized fragments, which were cleaned with acetone and isopropyl alcohol for 10 min, respectively. Then the lithography processes were performed to obtain electrodes of regular size and shape for current expansion. After that, the annealing process was carried out to make the nickel−gold alloy layer have both high transparency and electrical conductivity.

2.2. Fabrication of the Flexible (In,Ga)N Film and the Monolithic Device. The Sn/Pb alloy was melted to connect the Si and conducting wire with an electric soldering iron (Figure 1b). In order to avoid corrosion of the Sn/Pb alloy during the EC process, epoxy resin was used to cover the Sn/Pb alloy but expose wires. The Pt sheet and sample were immersed in 1 mol/L nitric acid (HNO_3) during the EC process solution, serving as the anode and cathode, respectively. Further details can be found in the refs 17,19. Before the transfer process, the silver paste was smoothed on the top surface of the indium−tin oxide (ITO) layer. After being detached from the Si substrate, the (In,Ga)N film was transferred to the surface of a silver paste. Then, the sample was kept at 130 °C for 30 min to solidify the silver paste.

2.3. Characterization and Measurement Methods. In order to characterize the photoelectric response, the PD characteristics were measured by using a semiconductor parameter measuring instrument (Agilent B1500A). The light-emitting diodes (LEDs) were used as lighting sources for the detection measurements. As a key parameter, the responsivity (R) of the PD is calculated by the following equation[20]

$$R = \frac{I_{ph}}{S_{device} \cdot P_{inc}} \quad (1)$$

P_{inc} is the incident optical power density, and I_{ph} is the optical response current. The effective area of the device (S_{device}) is 0.04 cm^2. Electroluminescence (EL) spectra were achieved by a current injection. To characterize the morphology and element distribution, spherical aberration-corrected scanning transmission electron microscopy (AC-STEM, Talos F200X, FEI) with high-resolution energy-dispersive X-ray (EDX) imaging was used.

https://doi.org/10.1021/acsomega.3c08503
ACS Omega 2024, 9, 8117−8122

3. RESULTS AND DISCUSSION

Figure 1c illustrates the distinct (In,Ga)N/GaN and (Al,Ga)-N/GaN interfaces within the (In,Ga)N/GaN MQWs, (Al,Ga) N EBL, and p-GaN areas, underscoring the agreement between the epitaxial structure and the design. Moreover, the distinct lattice fringes observed in (In,Ga)N and GaN crystals (Figure 1d−f) signify excellent crystallinity in the active region.

As the detection measurements can be accomplished at 0 V bias, the monolithic device is proposed to have the function of self-driven detection.[21−23] The photocurrent (I_{ph}) gradually increases with the increase in incident light−power intensity (P_{inc}), demonstrating a dependency on the light power (Figure 2a). When the P_{inc} is about 1.8 mW cm^{-2}, the responsivity (R) can reach 231.3 μA W^{-1} (Figure 2b). The limitation of the number of electron hole pairs in the device, coupled with the increase in carrier scattering and charge recombination rate caused by self-heating, results in the response current density tending to saturation.[24] According to eq 1, the increasing speed of I_{ph} is smaller than that of P_{inc}, leading to a decreased R (Figure 2b). The key parameters contain the rise time (t_{rise}) for the photocurrent increasing from 10 to 90% of its peak value and the decay time (t_{fall}) for that decreasing from 90 to 10%.[25,26] Figure 3c illustrates that the rise and fall times are 66 and 91 ms, respectively.

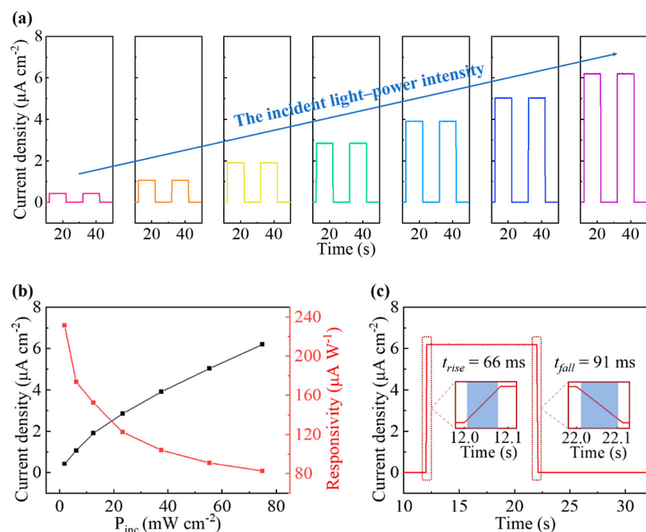

Figure 2. (a) Photoswitching behaviors of the monolithic bifunctional device under 365 nm illumination with different incident power densities. (b) Photocurrent density and responsivity as a function of the incident light-power density. (c) Photoresponse curve of the device under illumination at a zero-voltage bias.

In addition, to demonstrate the flexibility and stability of the self-driven PD, bending experiments of the device are completed, as shown in Figure 3a. When bending the PD under different curvature conditions, the clear and stable light-switching behavior can still be achieved (Figure 3b). Furthermore, the photocurrent density generated at a curvature (K) of 11.2 m^{-1} can remain about 68.3% of the photocurrent density generated in the flat state (Figure 3c). Therefore, the PD has good flexibility and stability in the bending states.

In order to characterize the luminous performance, the luminous power of the device under different bending states was measured, as shown in Figure 3a. The clear EL spectra demonstrate that the flexible device has another function of illumination (Figure 4a). When the bending curvature of the film increases from 0 to 11.2 m^{-1}, the cyan EL peak wavelength remains quite stable, only shifting 0.4 nm. In addition, the effective luminous area of the device is 0.094 cm^2. When the bending curvature of the substrate is 0, 7.9, and 11.2 m^{-1}, the luminous power is around 224.9, 145.4, and 134.7 μW cm^{-2}, respectively (Figure 4b). In other words, the optical power of the flexible device generated at the curvature of 11.2 m^{-1} can remain at about 60% of the maximum value generated in the flat state. Therefore, the flexible device can still have good luminous performance in a large bending state.

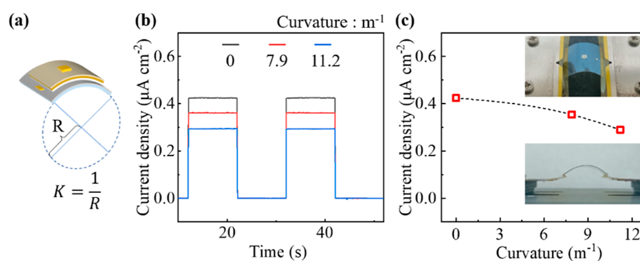

Figure 3. (a) Schematic bending model of the flexible bifunctional device. (b) Photoswitching behaviors of the flexible bifunctional device under 365 nm illumination under different bending states (K). (c) Photocurrent density of the device as a function of curvature (K) under illumination at a 0 V bias.

Figure 5 illustrates the schematic diagrams of the measurement models and energy bands of the (In,Ga)N films under irradiation. When external light radiation is applied (Figure 5a,b), the photogenerated electrons and holes begin to flow (Figure 5c). When the (In,Ga)N film is bent and then stimulated by UV pulses (Figure 5b), the piezoelectric charges can be generated at the ITO/(In,Ga)N interface,[27] causing the energy band to be bent upward (red curve in Figure 5d). This curved band state can result in slower carrier transport, resulting in a decrease in the optical responsivity (Figure 3c). When the forward bias is applied to the two electrodes of the device, electrons and holes are injected into the active region of the MQWs to emit light by combination (Figure 5e). It is clear that the transport directions of the detection and lighting processes are opposite. When we bend the (In,Ga)N film and then apply a forward bias, the same curved energy band state can slow down the carrier transport (Figure 5f), resulting in a decrease in the luminous power of the device (Figure 4b). Moreover, the removal of the epitaxial Si substrate by the EC method is beneficial for releasing stress, leading to reduce the internal polarization effects.[28] Hence, the EL peak wavelength can remain quite stable under bending conditions (Figure 4a).

To realize the two functions of detection and lighting at the same time, when the flexible device is in the detection state (Figure 5a), the forward bias is also applied to its two electrodes to make it emit light (Figure 6a). As clearly shown in Figure 6a, the flexible device can achieve an obvious optical switching response and stable luminescence, which proves that the device can successfully have stable detection performance even under a luminescence condition. In addition, under the stimulation with the same incident optical power densities, the direction of photocurrent under a luminescence condition is opposite to that under a nonluminescence condition. In order to investigate the relationship between the photocurrent direction and voltage, the device under a low voltage was measured (Figure 6b). When the voltage is very small (0.1 V),

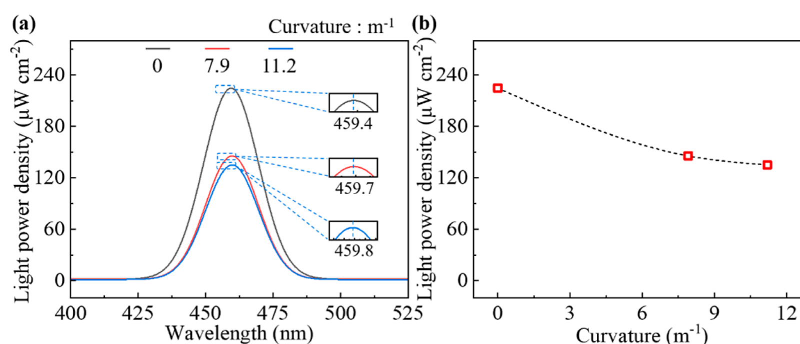

Figure 4. (a) EL spectra of the flexible monolithic device with different *K*. (b) Light power of the flexible bifunctional device with different *K*. To make it more accurate, the results are the average data of those measured three times.

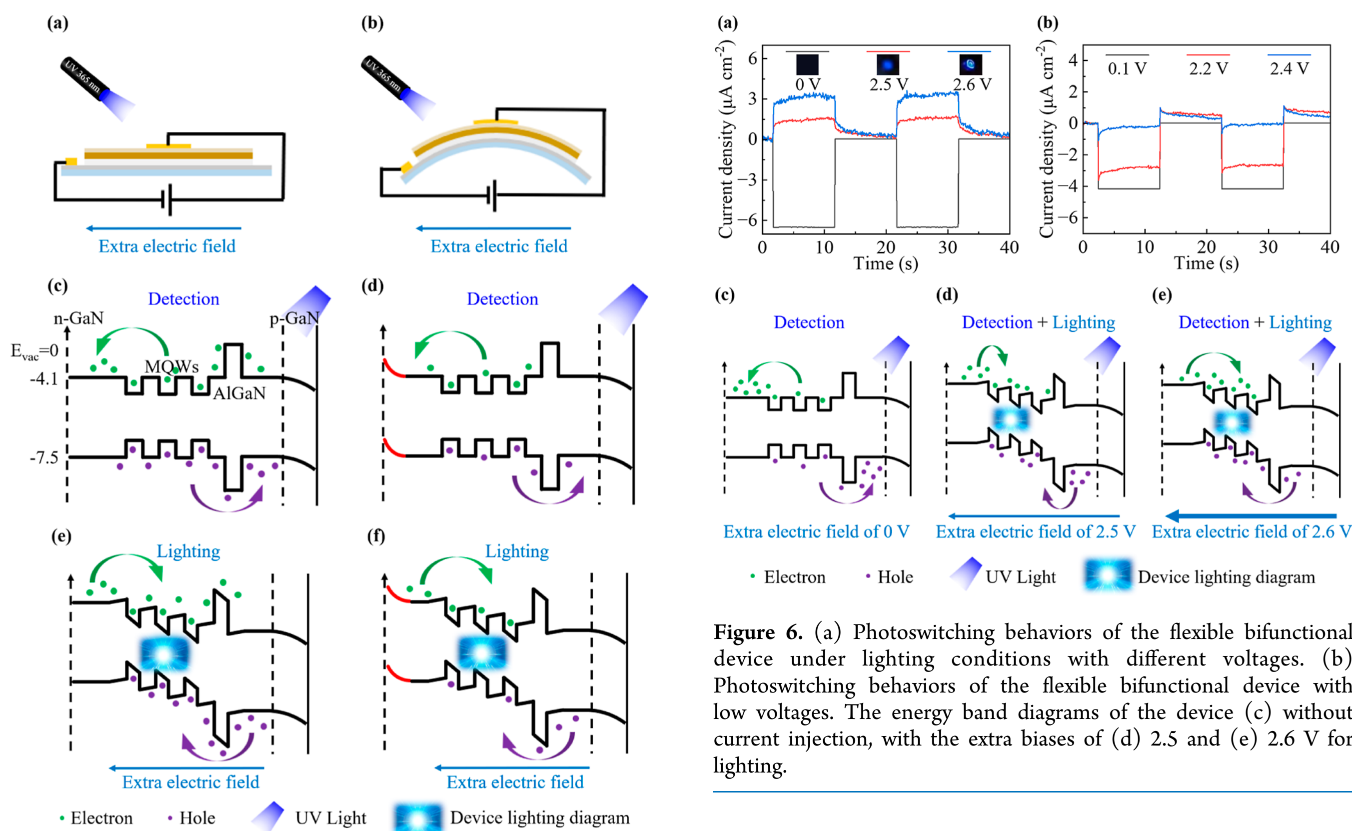

Figure 5. (a) Schematic diagram of measuring the flexible bifunctional device in the flat state. (b) Schematic diagram of measuring the flexible bifunctional device under bending. The energy band diagrams of (c) the flat device and (d) the bent device are obtained under illumination. The energy band diagrams of (e) the flat device and (f) the bent device under the current injection. For a clearer illustration, the 9-period (In,Ga)N/GaN MQWs are simplified as 3-period MQWs in the schematic energy band diagrams.

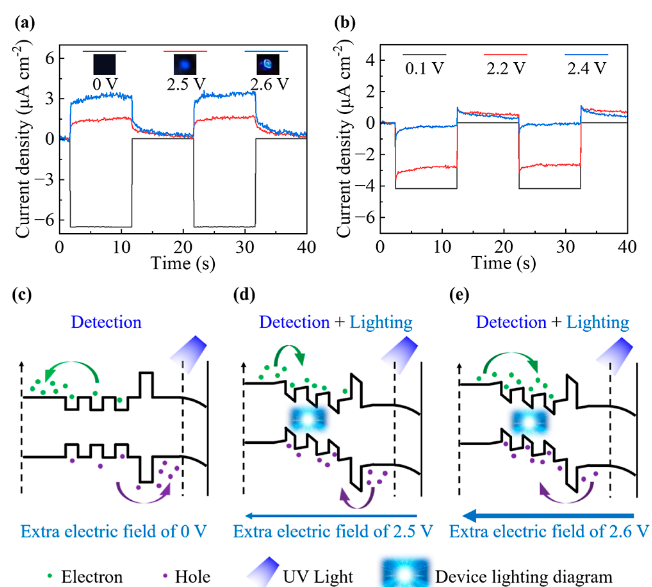

Figure 6. (a) Photoswitching behaviors of the flexible bifunctional device under lighting conditions with different voltages. (b) Photoswitching behaviors of the flexible bifunctional device with low voltages. The energy band diagrams of the device (c) without current injection, with the extra biases of (d) 2.5 and (e) 2.6 V for lighting.

the direction of the photocurrent is similar to that under 0 V bias. When the voltage is increased to 2.4 V, the photocurrent direction reaches a critical value. As the voltage continues to increase, the direction of the photocurrent will change from downward to upward. This is because under luminous conditions, the direction of the transport of electrons and holes in the device is affected by the applied electric field and the incident light. When the voltage is low, the impact of the incident light is greater, and the electrons and holes move normally (Figure 6c). When the voltage continues to increase, the effect of the applied electric field gradually increases to affect the movement direction of carriers, resulting in a change in the direction of the response current (Figure 6d). As the applied electric bias increases, more photogenerated electrons and holes are driven to produce a higher photocurrent (Figure 6e).

4. CONCLUSIONS

In this work, the (In,Ga)N film is detached from the original Si substrate by the EC method to realize a flexible monolithic bifunctional device successfully. Such a flexible device has both functions of emission and self-driven detection under different bending conditions. The EL peak wavelength of the device remains quite stable under different bending conditions, resulting from stress release and reduced internal polarization effects. Thanks to the good flexibility, the monolithic device can maintain both stable self-driven detection and emission performance under large bending condition. To meet the requirements of miniaturization and multifunctionality, the flexible monolithic device can perform two functions of

detection and lighting at the same time. Due to the requirements of affordability, compactness, and energy efficiency, the versatility of flexible monolithic bifunctional devices can extend to wearable solid-state lighting, communication, and monitoring applications.

■ ASSOCIATED CONTENT

Data Availability Statement

The data have already been provided in the form of excel. Further requested data can be made available upon publisher's request.

Supporting Information

The Supporting Information is available free of charge at https://pubs.acs.org/doi/10.1021/acsomega.3c08503.

Data underlying the results (XLSX)

■ AUTHOR INFORMATION

Corresponding Authors

Renjun Pei − *School of Nano-Tech and Nano-Bionics, University of Science and Technology of China, Hefei 230026, China; CAS Key Laboratory for Nano-Bio Interface, Suzhou Institute of Nano-Tech and Nano-Bionics (SINANO), Chinese Academy of Sciences (CAS), Suzhou 215123, China;* orcid.org/0000-0002-9353-3935; Email: rjpei2011@sinano.ac.cn

Yukun Zhao − *School of Nano-Tech and Nano-Bionics, University of Science and Technology of China, Hefei 230026, China; CAS Key Lab of Nanodevices and Applications, Suzhou Institute of Nano-Tech and Nano-Bionics (SINANO), Chinese Academy of Sciences (CAS), Suzhou 215123, China;* orcid.org/0000-0002-4071-4265; Email: ykzhao2017@sinano.ac.cn

Authors

Binbin Hou − *School of Nano-Tech and Nano-Bionics, University of Science and Technology of China, Hefei 230026, China; CAS Key Laboratory for Nano-Bio Interface, Suzhou Institute of Nano-Tech and Nano-Bionics (SINANO), Chinese Academy of Sciences (CAS), Suzhou 215123, China*

Qianyi Zhang − *CAS Key Lab of Nanodevices and Applications, Suzhou Institute of Nano-Tech and Nano-Bionics (SINANO), Chinese Academy of Sciences (CAS), Suzhou 215123, China*

Jianya Zhang − *Jiangsu Key Laboratory of Micro and Nano Heat Fluid Flow Technology and Energy Application, School of Physical Science and Technology, Suzhou University of Science and Technology, Suzhou 215009, China*

Complete contact information is available at: https://pubs.acs.org/10.1021/acsomega.3c08503

Author Contributions

B.B.H. completed all the experiments of device fabrication, device measurements, and the corresponding data collection and analysis. Y.K.Z. conceived the idea. Y.K.Z. and R.J.P. guided the work. B.B.H., R.J.P., and Y.K.Z. completed the mechanism study. Y.K.Z. and R.J.P. carried out the funding acquisition and project administration. B.B.H. and Y.K.Z. wrote the original draft of this work. B.B.H., Q.Y.Z., and J.Y.Z. carried out the methodology and visualization of this work. B.B.H., Q.Y.Z., and J.Y.Z. performed the investigation. All authors reviewed this manuscript.

Notes

The authors declare no competing financial interest.

■ ACKNOWLEDGMENTS

The authors are grateful for the Key Research Program of Frontier Sciences, CAS (no. ZDBS-LY-JSC034), the China Postdoctoral Science Foundation (nos. 2023TQ0238 and 2023M742560), and the National Natural Science Foundation of China (no. 62174172). The authors are thankful for the technical support for Nano-X, Platform for Characterization and Test from Suzhou Institute of Nano-Tech and Nano-Bionics, Chinese Academy of Sciences (SINANO).

■ REFERENCES

(1) Lu, X. Y.; Zhu, S. J.; Lin, R. Z.; Sun, D.; Cui, X. G.; Tian, P. F. Performance Improvement of Red InGaN Micro-LEDs by Transfer Printing From Si Substrate Onto Glass Substrate. *IEEE Electron Device Lett.* **2022**, *43* (9), 1491−1494.

(2) Morikawa, S.; Ueno, K.; Kobayashi, A.; Fujioka, H. Pulsed Sputtering Preparation of InGaN Multi-Color Cascaded LED Stacks for Large-Area Monolithic Integration of RGB LED Pixels. *Crystals* **2022**, *12* (4), 499.

(3) Zhu, S. J.; Shan, X. Y.; Qiu, P. J.; Wang, Z.; Yuan, Z. X.; Cui, X. G.; Zhang, G. Q.; Tian, P. F. Low-Power High-Bandwidth Non-Polar InGaN Micro-LEDs at Low Current Densities for Energy-Efficient Visible Light Communication. *IEEE Photonics J.* **2022**, *14* (5), 1−5.

(4) Ye, Z. Q.; Yan, J. B.; Gao, X. M.; Jia, B. L.; Guan, Q.; Fu, K.; Wang, L. N.; Zhu, H. B.; Ji, X. Y.; Wang, Y. J. Miniaturized III-Nitride Asymmetric Optical Link for the Monitoring of Vascular Heart Rate and Cardiac-Related Pulse Activity. *Adv. Eng. Mater.* **2022**, *24* (3), 2100829.

(5) Peng, L.; Hu, L.; Fang, X. Energy Harvesting for Nanostructured Self-Powered Photodetectors. *Adv. Funct. Mater.* **2014**, *24* (18), 2591−2610.

(6) Chang, S.; Zhao, Y.; Tang, J.; Bai, Z.; Zhao, L.; Zhong, H. Balanced Carrier Injection and Charge Separation of CuInS2 Quantum Dots for Bifunctional Light-Emitting and Photodetection Devices. *J. Phys. Chem. C* **2020**, *124* (12), 6554−6561.

(7) Wang, Y.; Wang, X.; Yuan, J.; Gao, X.; Zhu, B. Monolithic III-nitride photonic circuit towards on-chip optical interconnection. *Appl. Phys. Express* **2018**, *11* (12), 122201.

(8) Tsai, Y.-J.; Lin, R.-C.; Hu, H.-L.; Hsu, C.-P.; Wen, S.-Y.; Yang, C.-C. Novel Electrode Design for Integrated Thin-Film GaN LED Package With Efficiency Improvement. *IEEE Photonics Technol. Lett.* **2013**, *25* (6), 609−611.

(9) Bao, C.; Xu, W.; Yang, J.; Bai, S.; Teng, P.; Yang, Y.; Wang, J.; Zhao, N.; Zhang, W.; Huang, W.; et al. Bidirectional optical signal transmission between two identical devices using perovskite diodes. *Nat. Electron.* **2020**, *3* (3), 156−164.

(10) Li, K. H.; Fu, W. Y.; Cheung, Y. F.; Wong, K. K. Y.; Wang, Y.; Lau, K. M.; Choi, H. W. Monolithically integrated InGaN/GaN light-emitting diodes, photodetectors, and waveguides on Si substrate. *Optica* **2018**, *5* (5), 564−569.

(11) Jeong, H.; Cho, G. H.; Jeong, M. S. Redistribution of carrier localization in InGaN-based light-emitting diodes for alleviating efficiency droop. *J. Lumin.* **2022**, *252*, 119277.

(12) Zou, M.; Ma, Y.; Yuan, X.; Hu, Y.; Liu, J.; Jin, Z. Flexible devices: from materials, architectures to applications. *J. Semicond.* **2018**, *39* (1), 011010−011018.

(13) Baruah, R. K.; Yoo, H.; Lee, E. K. Interconnection Technologies for Flexible Electronics: Materials, Fabrications, and Applications. *Micromachines* **2023**, *14* (6), 1131.

(14) Gao, J.; Shang, K.; Ding, Y.; Wen, Z. Material and configuration design strategies towards flexible and wearable power supply devices: a review. *J. Mater. Chem. A* **2021**, *9* (14), 8950−8965.

(15) Wang, Y.; Yin, Q.; Ye, Z.; Fu, K.; Wang, H.; Su, Y.; Gao, X. Chip and Its Key Technology for Monolithically Integrated Visible

Light Communication and Sensing. *J. Electron. Inf. Technol.* **2022**, *44* (8), 2725−2729.

(16) Jiang, M.; Zhao, Y.; Zheng, P.; Zhang, J.; Yang, W.; Zhou, M.; Wu, Y.; Pei, R.; Lu, S. Flexible bidirectional self-powered photodetector with significantly reduced volume and accelerated response speed based on hydrogel and lift-off GaN-based nanowires. *Fundam. Res.* **2022**.

(17) Zhao, Y.; Xing, Z.; Geelhaar, L.; Zhang, J.; Yang, W.; Auzelle, T.; Wu, Y.; Bian, L.; Lu, S. Detaching (In,Ga)N Nanowire Films for Devices Requiring High Flexibility and Transmittance. *ACS Appl. Nano Mater.* **2020**, *3* (10), 9943−9950.

(18) Jiang, M.; Zhang, J.; Yang, W.; Wu, D.; Zhao, Y.; Wu, Y.; Zhou, M.; Lu, S. Flexible Self-Powered Photoelectrochemical Photodetector with Ultrahigh Detectivity, Ultraviolet/Visible Reject Ratio, Stability, and a Quasi-Invisible Functionality Based on Lift-Off Vertical (Al,Ga)N Nanowires. *Adv. Mater. Interfaces* **2022**, *9* (16), 2200028.

(19) Jiang, T.; Wang, J.; Liu, J.; Feng, M.; Yan, S.; Chen, W.; Sun, Q.; Yang, H. Lift-off of GaN-based LED membranes from Si substrate through electrochemical etching. *Appl. Phys. Express* **2022**, *15* (8), 086501.

(20) Fang, H. J.; Zheng, C.; Wu, L. L.; Li, Y.; Cai, J.; Hu, M. X.; Fang, X. S.; Ma, R.; Wang, Q.; Wang, H. Solution-Processed Self-Powered Transparent Ultraviolet Photodetectors with Ultrafast Response Speed for High-Performance Communication System. *Adv. Funct. Mater.* **2019**, *29* (20), 1809013.

(21) Zhang, H.; Ding, Q.; He, D.; Liu, H.; Liu, W.; Li, Z.; Yang, B.; Zhang, X.; Lei, L.; Jin, S. A p-Si/NiCoSex core/shell nanopillar array photocathode for enhanced photoelectrochemical hydrogen production. *Energy Environ. Sci.* **2016**, *9* (10), 3113−3119.

(22) May, M. M.; Lewerenz, H. J.; Lackner, D.; Dimroth, F.; Hannappel, T. Efficient direct solar-to-hydrogen conversion by in situ interface transformation of a tandem structure. *Nat. Commun.* **2015**, *6*, 8286.

(23) Son, M.-K.; Steier, L.; Schreier, M.; Mayer, M. T.; Luo, J.; Grätzel, M. A copper nickel mixed oxide hole selective layer for Au-free transparent cuprous oxide photocathodes. *Energy Environ. Sci.* **2017**, *10* (4), 912−918.

(24) Kong, W. Y.; Wu, G. A.; Wang, K. Y.; Zhang, T. F.; Zou, Y. F.; Wang, D. D.; Luo, L. B. Graphene-β-Ga_2O_3 Heterojunction for Highly Sensitive Deep UV Photodetector Application. *Adv. Mater.* **2016**, *28* (48), 10725−10731.

(25) Ma, D.; Zhao, J.; Wang, R.; Xing, C.; Li, Z.; Huang, W.; Jiang, X.; Guo, Z.; Luo, Z.; Li, Y.; et al. Ultrathin GeSe Nanosheets: From Systematic Synthesis to Studies of Carrier Dynamics and Applications for a High-Performance UV-Vis Photodetector. *ACS Appl. Mater. Interfaces* **2019**, *11* (4), 4278−4287.

(26) Jiang, M.; Zhao, Y.; Zhou, M.; Zhang, J.; Lu, S. Engineer carrier transport at (Al,Ga)N nanowire/hydrogel interface to realize self-driven ultraviolet photodetectors with switchable response speed for imaging system. *J. Alloys Compd.* **2023**, *966*, 171498.

(27) Waseem, A.; Johar, M. A.; Hassan, M. A.; Bagal, I. V.; Ha, J.-S.; Lee, J. K.; Ryu, S.-W. Effect of crystal orientation of GaN/V2O5 core-shell nanowires on piezoelectric nanogenerators. *Nano Energy* **2019**, *60*, 413−423.

(28) Dai, P.; Xu, Z. W.; Zhou, M.; Jiang, M.; Zhao, Y. K.; Yang, W. X.; Lu, S. L. Detach GaN-Based Film to Realize a Monolithic Bifunctional Device for Both Lighting and Detection. *Nanomaterials* **2023**, *13* (2), 359.

https://doi.org/10.1021/acsomega.3c08503
ACS Omega 2024, 9, 8117−8122